First-order superfluid to valence-bond solid phase transitions in easy-plane SU(N) magnets for small N

Jonathan D'Emidio and Ribhu K. Kaul

Phys. Rev. B **93**, 054406 — Published 3 February 2016

DOI: 10.1103/PhysRevB.93.054406

First-order superfluid to valence bond solid phase transitions in easy-plane SU(N) magnets for small-N

Jonathan D'Emidio and Ribhu K. Kaul

Department of Physics & Astronomy, University of Kentucky, Lexington, KY 40506-0055
(Dated: December 16, 2015)

We consider the easy-plane limit of bipartite SU(N) Heisenberg Hamiltonians which have a fundamental representation on one sublattice and the conjugate to fundamental on the other sublattice. For $N = 2$ the easy plane limit of the SU(2) Heisenberg model is the well known quantum XY model of a lattice superfluid. We introduce a logical method to generalize the quantum XY model to arbitrary N, which keeps the Hamiltonian sign-free. We show that these quantum Hamiltonians have a world-line representation as the statistical mechanics of certain tightly packed loop models of N-colors in which neighboring loops are disallowed from having the same color. In this loop representation we design an efficient Monte Carlo cluster algorithm for our model. We present extensive numerical results for these models on the two dimensional square lattice, where we find the nearest neighbor model has superfluid order for $N \leq 5$ and valence-bond order for $N > 5$. By introducing SU(N) easy-plane symmetric four-spin couplings we are able to tune across the superfluid-VBS phase boundary for all $N \leq 5$. We present clear evidence that this quantum phase transition is first order for $N = 2$ and $N = 5$, suggesting that easy-plane deconfined criticality runs away generically to a first order transition for small-N.

I. INTRODUCTION

Quantum phase transitions have emerged as an important paradigm in the study of quantum many-body phenomena.[1] Deconfined criticality is a novel field theoretic proposal for a continuous transition between a magnet or superfluid that breaks an internal symmetry and a valence bond solid (VBS) that breaks a lattice translational symmetry.[2,3] The field theories realized at these new critical points are strongly coupled gauge theories, which are rather fundamental and hence connected to a wide range of problems,[4,5] making the study of deconfined criticality of general interest in theoretical physics. The study of deconfined critical points has been significantly enhanced by the availability of sign problem free quantum Monte Carlo (QMC) simulations which are able to access the strong coupling physics of the emergent gauge theories in some particular Marshall positive Hamiltonians that host this phase transition.[6]

Historically, in the discovery of deconfined criticality, a prominent role was played by the "easy-plane" deconfined critical point, which is most naturally realized in lattice models of superfluids. The square lattice quantum XY model has been studied extensively in the last few decades as the simplest quantum lattice spin model for a superfluid. The model can be written in the following ways,

$$H_{XY} = -J \sum_{\langle ij \rangle} \left(S_i^x S_j^x + S_i^y S_j^y \right) \quad (1)$$

$$= -\frac{J}{2} \sum_{\langle ij \rangle} \left(S_i^+ S_j^- + S_i^- S_j^+ \right), \quad (2)$$

where the $\vec{S}_i$ are the usual $S = 1/2$ Pauli matrices on site i. The model has only a sub-group of the SU(2) symmetry of the Heisenberg model: it has a $U(1)$ rotation symmetry about the $\hat{z}$ axis and a Z_2 symmetry of flipping the S^z components. We note here that the sign of J is inconsequential, since it can be changed by a unitary transformation. The model H_{XY} is Marshall positive and hence free of the sign problem of quantum Monte Carlo. Exploiting this fact, extensive numerical simulations have shown that H_{XY} has long range superfluid order at $T = 0$. To study the destruction of superfluid order in the ground state, a sign-free generalization of the quantum XY model to include a four spin coupling K was introduced,[7]

$$H_K = -K \sum_{\langle ijkl \rangle} \left(S_i^+ S_j^- S_k^+ S_l^- + S_i^- S_j^+ S_k^- S_l^+ \right) \quad (3)$$

It has been shown that this model hosts three phases, a superfluid state at small K/J, valence-bond solid order for intermediate K/J and checkerboard ordered solid for large K/J. The phase transition between VBS and checkerboard was found (as expected) to be strongly first order. On the other hand the fate of the transition between superfluid and VBS in this model has remained enigmatic: while no evidence for a discontinuity have been observed in this model, large scaling violations may not be interpreted consistently as a continuous transition.[8] This transition if continuous would be the first studied example of a "deconfined critical point," its first numerical study[7] even predating the field theoretic proposal.[2] The square lattice easy-plane model played a prominent role in the original deconfined critical point proposal. Additionally it has been shown that should the superfluid-VBS transition in the quantum XY model be continuous, it would be a rare example of a self-dual critical point,[9] which can be connected to various interesting field theoretic formulations with topological terms.[10] We note here that some direct studies of the effective field

theory[11,12] and other quantum models on frustrated lattices[13,14] which are believed to be in the same universality class have found evidence for a first order transition. In the meantime, attention in deconfined criticality has shifted to the study of the fully SU(N) symmetric Hamiltonians,[15–17] and more recently loop models,[18] which have shown compelling evidence for a continuous transition.

However, given the important role that the square lattice XY model has had as the first putative host of deconfined criticality, it remains of interest to have an unambiguous answer to the nature of the superfluid-VBS transition in this model. Instead of addressing this issue in the J-K model, where the results of the simulations are hard to interpret[8] we study a different model which can be understood as an easy-plane generalization of the SU(2) symmetric J-Q model.[15] We provide clear evidence that the transition in this model is direct and discontinuous both for superfluid and the VBS order. Additionally, we are able to provide a simple way to generalize the easy-plane J-Q model to larger-N. Through large scale numerical simulations we show that $H^N_{J_\perp Q_\perp}$ hosts the superfluid-VBS phase transition for all $N \leq 5$. We provide evidence that this transition remains first order for $N = 5$, which leads us to conclude that easy-plane deconfined criticality is generically first order for small-N.

The paper is organized as follows. In Sec. II, we introduce the new easy-plane J-Q model, $H^N_{J_\perp Q_\perp}$ and write it down in different ways, emphasizing how it is connected to previously studied models. In Sec. III we show how it maps to a particular family of loop models in one higher dimension and use this representation to formulate an efficient Monte Carlo algorithm. In Sec. IV, we present results of simulations of $H^N_{J_\perp Q_\perp}$ on the square lattice, focusing on the first-order nature of the phase transitions in this model. Finally, in Sec. V, we provide our conclusions and outlook.

II. LATTICE HAMILTONIANS

It is useful to write our Hamiltonian in a few different ways to elucidate certain diverse aspects. First let us consider the generalization of the XY model in the form, Eq. (1) to arbitrary-N. A natural way to do this on a bipartite lattice in the spirit of the work of Affleck,[19] is to consider the following Hamiltonian,

$$H^N_{J_\perp} = -\frac{J_\perp}{N} \sum_{\langle ij \rangle} \sum_{a \in od} T^a_i T^{a*}_j, \tag{4}$$

where the T_i are $N \times N$ matrices acting on site i, which are the generators of SU(N). Here we choose the normalization such that $\mathrm{Tr}[T^a T^b] = \delta_{ab}$. These generators act on a local Hilbert space which now can take N different colors and are denoted by $|\alpha\rangle_i$. We note that i is always chosen on the A sub-lattice and j is chosen on the B sub-lattice, so that spins on one sublattice transform in the fundamental and spins on the other sublattice transform under the conjugate to fundamental representations. The important difference with the usual fully SU(N) symmetric Heisenberg model is the sum on generators a, is restricted to the off-diagonal generators. We note also that Eq. (1) is equivalent to Eq. (4) for $N = 2$ up to a unitary transformation about S^y on one sublattice. It is well known that of the $N^2 - 1$ generators of SU(N), $N - 1$ are diagonal and $N^2 - N$ are off-diagonal. The restriction of the sum to the $N^2 - N$ off diagonal generators guarantees that when $N = 2$, we recover the usual XY model. For larger N, Eq. (4) is a convenient large N generalization of the XY model. We note here that the restriction to off-diagonal generators reduces the symmetry from SU(N) to an Abelian $\mathrm{U}(1)^{N-1} \times \mathrm{S}_N$ subgroup (where S_N is the permutation group), which generalizes the $\mathrm{U}(1) \times \mathrm{Z}_2$ of Eq. (1). Physically this corresponds to rotations about the directions of the $N - 1$ diagonal generators and a discrete relabeling of the colors. We shall call this symmetry ep-SU(N) symmetry. Just like in the fully symmetric SU(N) case, the virtue of staggering the representation is that an A-B pair can form an ep-SU(N) singlet for all N. For sites $i \in A$ and $j \in B$, the singlet may be written as $|s_{ij}\rangle = \frac{1}{\sqrt{N}} \sum_{\alpha=1}^{N} |\alpha_i \alpha_j\rangle$

Having written the model formally in terms of the SU(N) generators helps us see that model is a large-N extension of H_{XY}. To get a better intuition for the matrix elements of the model we now write it directly in terms of the local Hilbert space. In terms of which, Eq. (4) takes the simple form,

$$H^N_{J_\perp} = -\frac{J_\perp}{N} \sum_{<ij>} \tilde{P}_{ij} \tag{5}$$

$$\tilde{P}_{ij} = \sum_{\alpha,\beta=1,\alpha\neq\beta}^{N} |\beta\beta\rangle_{ij} \langle\alpha\alpha|_{ij}. \tag{6}$$

We have put a tilde on $\tilde{P}_{ij}$ to emphasize that it is not a projection operator. It would have been the SU(N) symmetric projector on the singlet state $|s\rangle_{ij}$ if the condition $\alpha \neq \beta$ were dropped. Having $\alpha \neq \beta$ in $\tilde{P}_{ij}$ is a direct consequence of restricting the sum on a in Eq. (4) to off-diagonal generators and is what results in the reduced easy-plane symmetry. This form of the Hamiltonian also makes it apparent that the model is Marshall positive (off-diagonal matrix elements are all negative) and is hence amenable to sign problem free quantum Monte Carlo, just like the fully SU(N) symmetric case.[20]

Now it is straightforward to extend the idea of a four-spin coupling, the so called "Q" interaction[15,16] to the easy-plane case for any N,

$$H^N_{Q_\perp} = -\frac{Q_\perp}{N^2} \sum_{<ijkl>} \tilde{P}_{ij} \tilde{P}_{kl}, \tag{7}$$

where as in the original J-Q model, the sum is taken on both orientations of the bond pairing of the square

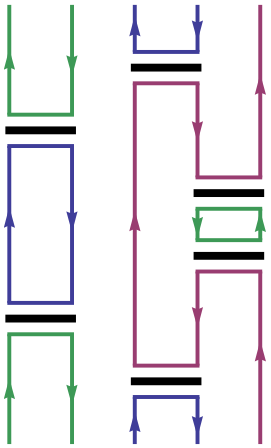

FIG. 1: A section of a stochastic series expansion configuration of the Hamiltonian, Eq. (5), which takes a simple form in terms of N-colored tightly packed oriented closed loops. By "oriented", we mean an orientation of the links (e.g. shown here as arrows going up on the A sub-lattice and down on the B sub-lattice) can be assigned before any loops are grown, and the orientation remains unviolated by each of the loops in a configuration. The extreme easy-plane anisotropy results in an important constraint, *i.e.* loops that share a vertex (operators represented by the black bars) are restricted to have different colors.

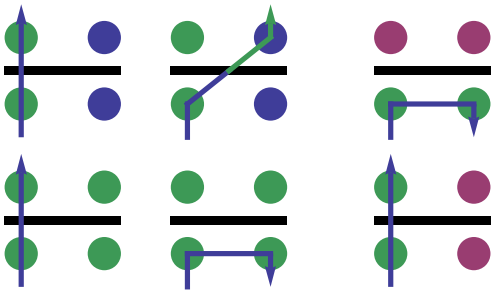

(a) Moves with probability 1/2 (b) Moves with probability 1

FIG. 2: Loop updating moves describing how loops pass through a vertex, depicted with a black bar. These moves cause conversions between the diagonal and off-diagonal matrix elements present in the Hamiltonian. For each update pictured here there is a reverse process that we have not drawn.

lattice plaquettes. We note here that for $N = 2$, the $Q_\perp$ term does *not* reduce to H_K, Eq. (3). It includes all the terms present there, but contains in addition pair hopping terms that are not present in H_K. Thus $H^N_{J_\perp Q_\perp} \equiv H^N_{J_\perp} + H^N_{Q_\perp}$ provides a new way to cross the superfluid-VBS phase boundary for $N = 2$ and also provides a neat way to extend the four spin interaction to arbitrary N, while still preserving the desired ep-SU(N) symmetry.

III. LOOP REPRESENTATION AND ALGORITHM

It turns out that our models has a convenient world-line representation in terms of closed loops in one higher dimension. While allowing us to design an efficient algorithm, it also allows us to connect our work to recent numerical studies of deconfined criticality in loop models.[18]

To see this start with Eq. (5) and construct a stochastic series expansion (see Ref. [21] for a comprehensive review). From previous work on similar models (see e.g. Ref. [22]), we know that the partition function of SU(N) quantum spin Hamiltonians can be viewed as the classical statistical mechanics of N-colors of tightly packed oriented loops in one higher dimension (see also[23]). A section of this particular kind of loop configuration, describing one term in the expansion of the partition function is depicted in FIG. 1 for our model. An essential difference from the usual SU(N) case (and the loop models studied so far[18,23]) is that loops which are attached to the same vertex (operators represented by the black bars) are restricted to have different colors, which is due to the absence of diagonal matrix elements in Eq. (5). This adds an important constraint: whereas in the fully symmetric SU(N) case, given a legal loop configuration loop colors could be assigned independently, in the easy-plane case studied here only a subset of the colorings (the ones that respect the constraint) are allowed. This affects profoundly the physics of the easy-plane model, as well as the recoloring of loops in a Monte-Carlo algorithm.

The fact that the loops in our model obey a coloring constraint and that diagonal operators are absent makes this model difficult to simulate as given. This difficulty is overcome, as is commonly done, by shifting the Hamiltonian by a constant. We shift our Hamiltonian in such a way that we introduce diagonal operators with equal weight as the off-diagonal ones. This shift only adds a constant to the energies and does not affect the physics of the model in anyway, i.e. the eigenstates are identical. The shifted Hamiltonian is given by

$$\tilde{H}^N_{J_\perp} = -\frac{J_\perp}{N} \sum_{<ij>} (\tilde{P}_{ij} + \mathbb{1}) \tag{8}$$

where the diagonal and off-diagonal operators have equal weight. With this shift the directed loop equations [24], describing how the loops pass through a vertex, take on a particularly simple form. We show the loop updating moves and corresponding probabilities in Fig. 2. With these rules the loops used to update our QMC configurations are not deterministic, as they are in the SU(N) symmetric case. The loops here can intersect with themselves and one may worry about growing a loop that fails to close onto itself. We have never seen a case of a loop not closing during any of our simulations.

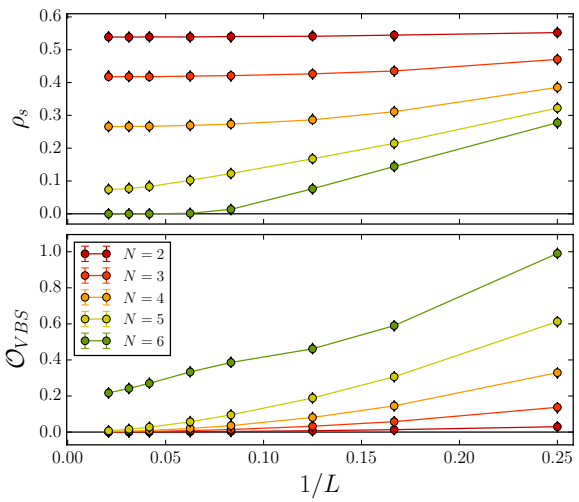

FIG. 3: The stiffness and VBS order parameter extrapolations as a function of $1/L$ for different N in the nearest neighbor easy-plane model $H^N_{J_\perp}$, defined in Eq. (4) or equivalently (5). We find clear evidence that the system has superfluid order for all $N \leq 5$ and VBS order for $N > 5$. To show ground state convergence we plot both $\beta = L, 2L$ in diamond and circular points, respectively.

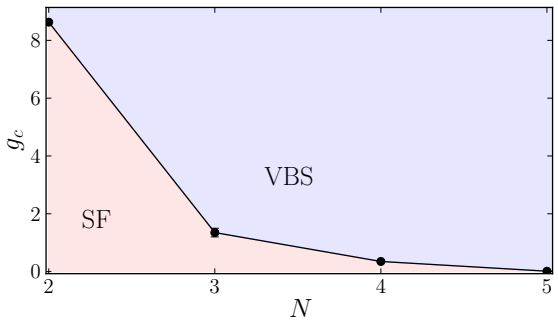

FIG. 4: Phase diagram of the $H^N_{J_\perp Q_\perp}$ model as a function of the ratio $g_c = Q_\perp/J_\perp$ and N. Using the $H^N_{J_\perp Q_\perp}$ model we have access to the superfluid-VBS phase boundary for $N = 2, 3, 4$ and 5. In this work, we provide clear evidence that the transition for $N = 2$ and $N = 5$ is direct but discontinuous for both order parameters, suggesting that the easy-plane-SU(N) superfluid-VBS transition is generically first order for small-N.

So far we have described our algorithm with $Q_\perp = 0$. The introduction of plaquette operators is easily dealt with if we regard them as simply a product of two (shifted) bond operators. Our algorithm then inserts and removes diagonal plaquette operators, present due to the constant shift, and can convert them to off-diagonal plaquettes by performing loop updates. Since the plaquette operator is viewed as two separate bonds operators, loop updates through the former are the same as for the latter.

IV. RESULTS OF NUMERICAL SIMULATIONS

A. MEASUREMENTS

Here we will outline the measurements that we use to characterize the phases of our model. On the magnetic side of the transition the spin stiffness, or superfluid stiffness in the language of hard-core bosons, serves as a useful order parameter. It is formally defined as follows:

$$\rho_s = \frac{1}{N_{\text{site}}} \frac{\partial^2 \langle H(\phi) \rangle}{\partial \phi^2}\Big|_{\phi=0} \tag{9}$$

where $H(\phi)$ means that we twist the boundary conditions along either the x or y direction. This twist can be implemented, for instance, by attaching phase factors to all x-oriented bond operators relative to one color e.g. $e^{i\phi}|\alpha\alpha\rangle_{ij}\langle \bigcirc\bigcirc|_{ij}$ for $\alpha \neq \bigcirc$, $i \in A$ sublattice and $j \in B$ sublattice. The Hermitian conjugate of this operator appears with $e^{-i\phi}$. Due to the staggered representation, the signs in the exponent are flipped when $i \in B$ and $j \in A$.

The bond operators take on this form when the spins are incrementally twisted along the x-direction about the $N-1^{\text{th}}$ diagonal generator of SU(N). In practice, due to the permutation symmetry of the model, the $\bigcirc$ color is arbitrary, and we can average over the colors in QMC.

In QMC the stiffness is related to the winding number of configurations via

$$\rho_s = \frac{1}{N_{\text{site}}} \frac{\langle W^2 \rangle}{\beta}, \tag{10}$$

where operators with a positive (negative) phase factor count as positive (negative) winding.

In order to characterize the VBS phase, we measure the equal time bond-bond correlation function $\langle \tilde{P}_{\vec{r}\alpha} \tilde{P}_{\vec{r}'\alpha} \rangle$. Here we have denoted a bond by its location on the lattice $\vec{r}$ and its orientation α (x or y in two-dimensions). In the VBS phase, lattice translational symmetry is broken giving rise to a Bragg peak in the Fourier transform of the bond-bond correlator defined as

$$\tilde{C}^\alpha(\vec{q}) = \frac{1}{N^2_{\text{site}}} \sum_{\vec{r},\vec{r}'} e^{i(\vec{r}-\vec{r}')\cdot\vec{q}} \langle \tilde{P}_{\vec{r}\alpha} \tilde{P}_{\vec{r}'\alpha} \rangle. \tag{11}$$

For columnar VBS patterns, peaks appear at the momenta $(\pi, 0)$ and $(0, \pi)$ for x and y-oriented bonds, respectively. The VBS order parameter is thus given by

$$\mathcal{O}_{VBS} = \frac{\tilde{C}^x(\pi, 0) + \tilde{C}^y(0, \pi)}{2}. \tag{12}$$

Another useful quantity that we use to locate phase transitions is the VBS ratio.

$$\mathcal{R}^x_{VBS} = 1 - \tilde{C}^x(\pi + 2\pi/L, 0)/\tilde{C}^x(\pi, 0) \tag{13}$$

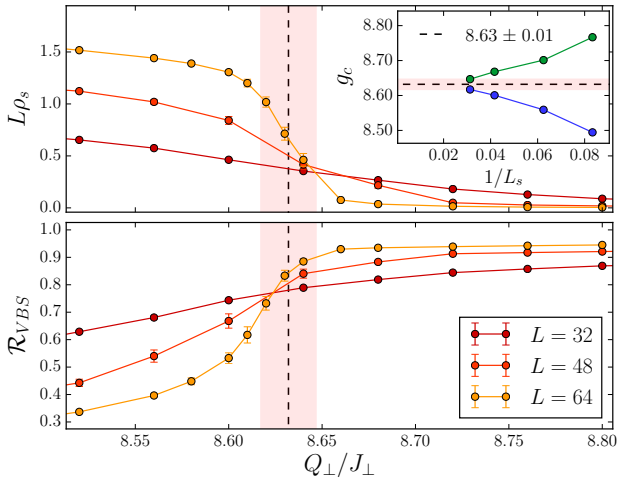

FIG. 5: Crossings at the SF-VBS quantum phase transition for $N = 2$ in $H^N_{J_\perp Q_\perp}$. The main panels shows the crossings for $L\rho_s$ and $\mathcal{R}_{VBS}$, which signal the destruction and onset of SF and VBS order respectively. The inset shows that the SF-VBS transition is direct, i.e. the destruction of SF order is accompanied by the onset of VBS order at a coupling of $g_c = 8.63(1)$.

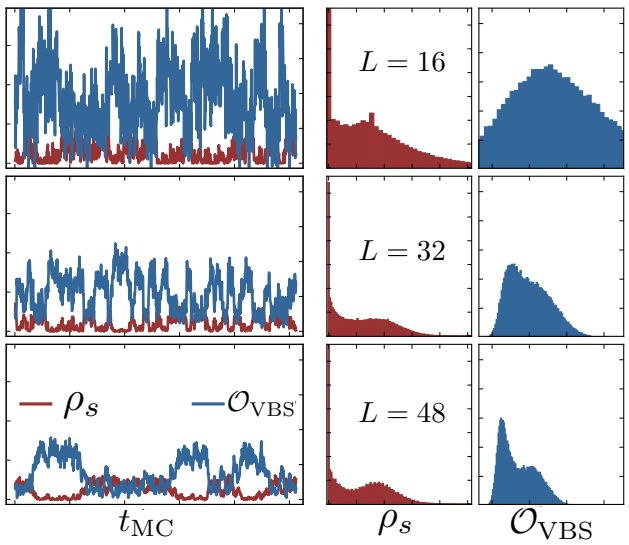

FIG. 6: Evidence for first order behavior at the SF-VBS quantum phase transition for $N = 2$. The data was collected at a coupling $g_c = 8.63$. The left panel shows MC histories for both ρ_s and $\mathcal{O}_{VBS}$, with clear evidence for switching behavior characteristic of a first order transition. The right panel shows histograms of the same quantities with double peaked structure which gets stronger with system size, again clearly indicating a first order transition. The bin size for the histories is 400 MC steps per point

And similarly for $\mathcal{R}^y_{VBS}$ with all of the q_x and q_y arguments swapped. We then average over x and y- orientations.

$$\mathcal{R}_{VBS} = \frac{\mathcal{R}^x_{VBS} + \mathcal{R}^y_{VBS}}{2}. \tag{14}$$

This quantity goes to 1 in a phase with long-range VBS order, and approaches 0 in a phase without VBS order. It is thus a useful crossing quantity that allows us to locate the transition.

To construct these quantities, we measure the equal time bond-bond correlation function in QMC with the following estimator

$$\langle \Theta_1 \Theta_2 \rangle = \frac{1}{\beta^2} \langle (n-1)! N[\Theta_1, \Theta_2] \rangle \tag{15}$$

where Θ_1 and Θ_2 are any two QMC operators (in our case off-diagonal bond operators), n is the number of non-null operators in the operator string, and $N[\Theta_1, \Theta_2]$ is the number of times Θ_1 and Θ_2 appear in sequence in the operator string (excluding null slots).

B. $J_\perp$-only model

Consider the ground state phase of $H^N_{J_\perp}$ as we vary the number of colors N. For $N = 2$ we know the Hamiltonian is equivalent to the quantum XY model, whose ground state is a superfluid. Here it is useful to recall our interpretation of $H^N_{J_\perp}$ as a classical loop model, discussed in Sec. III. In the loop language this corresponds to a long loop phase, where the loops span the system. It is expected that when N is increased the system would like to form as many loops as possible to maximize its entropy, causing it to enter a short loop phase. The way our loop model is defined this will cause the lattice symmetry to break, leading to a VBS and destruction of superfluid order.

Motivated by these considerations, in FIG. 3 we plot the spin-stiffness and VBS order parameter for $2 \leq N \leq 6$. We find that the ground state of this Hamiltonian has long-range superfluid order for $N \leq 5$ (signaled by a finite spin stiffness) and has VBS order for $N > 5$. These results are obtained by fixing $J_\perp = N, Q_\perp = 0$ and we have plotted two values of inverse temperature $\beta = L, 2L$. On the scale of the plot the two values of β are indistinguishable thus indicating ground state convergence. Since we find magnetic order for $N \leq 5$, we can study the phase transition for these values of N with the introduction of $Q_\perp$.

In conclusion, we find that magnetic order gives way to VBS order in the ep-SU(N) magnet at an N between 5 and 6. In comparison, in the fully SU(N) symmetric case magnetic order is lost between $N = 4$ and 5.[20,25]

C. $J_\perp$-$Q_\perp$ model

Through numerical simulations described below we have obtained a phase diagram of the model $H^N_{J_\perp Q_\perp}$, which we show in FIG. 4. It is clear that the $Q_\perp$ interaction, which mediates an attraction between the sin-

glets will favor the formation of a VBS state. We confirm this by numerical simulations in which we find that the superfluid order is destroyed at a finite value of $Q_\perp$ for $N = 2$ and gives way to a VBS state. As we increase N, the superfluid order becomes weaker in $H^N_{J_\perp}$, hence requiring only a smaller value of the $Q_\perp$ coupling to destroy the SF order, as is evident from the phase diagram. A significant difference from the phase diagram[7] of the J-K model, Eq. (3), is the absence of the checkerboard ordered state at large $Q_\perp$, which is present for large K. This can be expected on physical grounds by a comparison of the $Q_\perp$ and K terms. Finally, as expected for $N > 5$, we are unable to cross the superfluid-VBS phase boundary with $H^N_{J_\perp Q_\perp}$.

We now turn to an analysis of the quantum phase transitions which are denoted by the solid black points in FIG. 4. We begin with the case of $N = 2$. FIG. 5 shows SU(2) data of our magnetic and VBS crossing quantities, $L\rho_s$ and $\mathcal{R}_{VBS}$. In our data scans we have fixed $J_\perp^2 + Q_\perp^2 = 1$ and have set $\beta = 2L$. Our best estimate for the location of the transition is $Q_\perp/J_\perp = 8.63(1)$. Close to the transition we find that signs of first-order behavior begin to appear. FIG. 6 shows the histories of our measurements as a function of Monte Carlo time. We find clear signs that our measurements switch between two values close the transition, an effect which becomes more pronounced at larger system size. Furthermore, binning this data into histograms shows a clear double peaked structure, indicating a first order transition (FIG. 6).

It is interesting to ask whether the first order behavior observed is special to $N = 2$. Given the self-duality of $N = 2$,[9] which cannot be extended to $N > 2$, it is possible that the nature of the phase transition is different for other values of N. To investigate this issue we have carried out a full numerical study of $N = 5$, the largest value of N at which the SF-VBS transition is accessible in our model, $H^N_{J_\perp Q_\perp}$. We find first order behavior for $N = 5$ very similar to what we have presented here for $N = 2$. Numerical results and an analysis are presented in Appendix B. This leads us to conclude that the first-order behavior is not special to $N = 2$, but is present generically at small-N in our ep-SU(N) models.

V. CONCLUSIONS

To summarize, we have introduced a new family of ep-SU(N) models which generalize the XY model of $N = 2$. The generalization preserves the property that it takes only two sites to form a singlet, independent of the value of N. This property is important to the formation of a columnar VBS state. The generalization defines an easy-plane four-spin interaction $Q_\perp$, which allows us to access the superfluid-VBS phase boundary for $N = 2, 3, 4$ and 5. Numerical studies show clear evidence for first order behavior.

How should this observation be interpreted in the terms of the field theoretic picture of deconfined criticality? In the deconfined criticality scenario the first order transition could either be because the field theory itself does not have a fixed point or because the field theoretic fixed point is unstable to the introduction of quadrupled monopoles (i.e. they are relevant at the fixed point in the renormalization group sense).[26] Given the original arguments for irrelevance[3] and the numerical evidence in the symmetric case that quadrupled monopoles are irrelevant, we interpret the observed first order behavior here to imply that the non-compact easy-plane deconfined field theory itself is unstable to runaway flow for small-N. This is consistent with direct numerical studies of the easy-plane theory for $N = 2$.[11,12] Our study raises questions that need to be addressed in future field theoretic and numerical work. Is there a stable large-N easy-plane SU(N) deconfined critical point, or is there a generic reason it does not exist? If it does exist, it is interesting to ask whether numerical simulations will be able to access a large enough N to study this new quantum criticality.

Another interesting topic is the nature of the transition in the ep-SU(N) *without* Berry phases. This study can be numerically achieved by studying our model, Eq. (4) on a bilayer square lattice. For $N = 2$ one would expect a 3D XY transition – what happens at larger-N? Previous work on the bilayer SU(N) magnet[27] and classical loop models[28] has shown in the symmetric case that the transition is first order for large enough N, the answer to the same question in the easy-plane case is not known currently and will be pursued in future work.

Acknowledgements: We acknowledge useful discussion with G. Murthy. Partial financial support was received through NSF DMR-1056536. The numerical simulations reported in the manuscript were carried out on the DLX cluster at the University of Kentucky.

[1] S. Sachdev, *Quantum Phase Transitions* (Cambridge University Press, 1999).
[2] T. Senthil, A. Vishwanath, L. Balents, S. Sachdev, and M. P. A. Fisher, Science **303**, 1490 (2004), URL http://www.sciencemag.org/content/303/5663/1490.abstract.
[3] T. Senthil, L. Balents, S. Sachdev, A. Vishwanath, and M. P. A. Fisher, Phys. Rev. B **70**, 144407 (2004), URL http://link.aps.org/doi/10.1103/PhysRevB.70.144407.
[4] B. I. Halperin, T. C. Lubensky, and S.-k. Ma, Phys. Rev. Lett. **32**, 292 (1974), URL http://link.aps.org/doi/10.1103/PhysRevLett.32.292.
[5] A. Vishwanath and T. Senthil, Phys. Rev. X **3**, 011016 (2013), URL http://link.aps.org/doi/10.1103/

PhysRevX.3.011016.
[6] R. K. Kaul, R. G. Melko, and A. W. Sandvik, Annu. Rev. Cond. Matt. Phys **4**, 179 (2013), URL http://www.annualreviews.org/doi/abs/10.1146/annurev-conmatphys-030212-184215.
[7] A. W. Sandvik, S. Daul, R. R. P. Singh, and D. J. Scalapino, Phys. Rev. Lett. **89**, 247201 (2002), URL http://link.aps.org/doi/10.1103/PhysRevLett.89.247201.
[8] A. W. Sandvik and R. Melko, *Nature of the antiferromagnetic to valence-bond-solid quantum phase transition in a 2d xy-model with four-site interactions* (2006), URL http://arxiv.org/abs/cond-mat/0604451.
[9] O. I. Motrunich and A. Vishwanath, Phys. Rev. B **70**, 075104 (2004), URL http://link.aps.org/doi/10.1103/PhysRevB.70.075104.
[10] T. Senthil and M. P. A. Fisher, Phys. Rev. B **74**, 064405 (2006), URL http://link.aps.org/doi/10.1103/PhysRevB.74.064405.
[11] A. Kuklov, N. Prokofev, B. Svistunov, and M. Troyer, Annals of Physics **321**, 1602 (2006), ISSN 0003-4916, july 2006 Special Issue, URL http://www.sciencedirect.com/science/article/pii/S0003491606000789.
[12] S. Kragset, E. Smørgrav, J. Hove, F. S. Nogueira, and A. Sudbø, Phys. Rev. Lett. **97**, 247201 (2006), URL http://link.aps.org/doi/10.1103/PhysRevLett.97.247201.
[13] S. V. Isakov, S. Wessel, R. G. Melko, K. Sengupta, and Y. B. Kim, Phys. Rev. Lett. **97**, 147202 (2006), URL http://link.aps.org/doi/10.1103/PhysRevLett.97.147202.
[14] A. Sen, K. Damle, and T. Senthil, Phys. Rev. B **76**, 235107 (2007), URL http://link.aps.org/doi/10.1103/PhysRevB.76.235107.
[15] A. W. Sandvik, Phys. Rev. Lett. **98**, 227202 (2007), URL http://link.aps.org/doi/10.1103/PhysRevLett.98.227202.
[16] J. Lou, A. W. Sandvik, and N. Kawashima, Phys. Rev. B **80**, 180414 (2009), URL http://link.aps.org/doi/10.1103/PhysRevB.80.180414.
[17] R. K. Kaul and A. W. Sandvik, Phys. Rev. Lett. **108**, 137201 (2012), URL http://link.aps.org/doi/10.1103/PhysRevLett.108.137201.
[18] A. Nahum, J. T. Chalker, P. Serna, M. Ortuño, and A. M. Somoza, *Deconfined quantum criticality, scaling violations, and classical loop models* (2015), URL http://arxiv.org/abs/1506.06798.
[19] I. Affleck, Phys. Rev. Lett. **54**, 966 (1985), URL http://link.aps.org/doi/10.1103/PhysRevLett.54.966.
[20] K. Harada, N. Kawashima, and M. Troyer, Phys. Rev. Lett. **90**, 117203 (2003), URL http://journals.aps.org/prl/abstract/10.1103/PhysRevLett.90.117203.
[21] A. W. Sandvik, AIP Conf. Proc. **1297**, 135 (2010), URL http://scitation.aip.org/content/aip/proceeding/aipcp/10.1063/1.3518900.
[22] R. K. Kaul, Phys. Rev. B **91**, 054413 (2015), URL http://link.aps.org/doi/10.1103/PhysRevB.91.054413.
[23] A. Nahum, J. T. Chalker, P. Serna, M. Ortuño, and A. M. Somoza, Phys. Rev. Lett. **107**, 110601 (2011), URL http://link.aps.org/doi/10.1103/PhysRevLett.107.110601.
[24] O. F. Syljuåsen and A. W. Sandvik, Phys. Rev. E **66**, 046701 (2002).
[25] K. S. D. Beach, F. Alet, M. Mambrini, and S. Capponi, Phys. Rev. B **80**, 184401 (2009), URL http://link.aps.org/doi/10.1103/PhysRevB.80.184401.
[26] M. S. Block, R. G. Melko, and R. K. Kaul, Phys. Rev. Lett. **111**, 137202 (2013), URL http://link.aps.org/doi/10.1103/PhysRevLett.111.137202.
[27] R. K. Kaul, Phys. Rev. B **85**, 180411 (2012), URL http://link.aps.org/doi/10.1103/PhysRevB.85.180411.
[28] A. Nahum, J. T. Chalker, P. Serna, M. Ortuño, and A. M. Somoza, Phys. Rev. B **88**, 134411 (2013), URL http://link.aps.org/doi/10.1103/PhysRevB.88.134411.

Appendix A: QMC vs ED

4×4	$N=2$	$J_\perp=1.0$	$Q_\perp=0.0$	$\beta_{\rm qmc}=48.0$	
$e_{\rm ex}$	-0.562486	$\rho_{\rm ex}$	0.27714	$\mathcal{O}_{\rm ex}$	0.007497
$e_{\rm qmc}$	$-0.562473(7)$	$\rho_{\rm qmc}$	0.27710(3)	$\mathcal{O}_{\rm qmc}$	0.007497(1)
4×4	$N=2$	$J_\perp=1.0$	$Q_\perp=1.0$	$\beta_{\rm qmc}=32.0$	
$e_{\rm ex}$	-0.741775	$\rho_{\rm ex}$	0.35858	$\mathcal{O}_{\rm ex}$	0.011097
$e_{\rm qmc}$	$-0.741770(8)$	$\rho_{\rm qmc}$	0.35860(3)	$\mathcal{O}_{\rm qmc}$	0.011096(1)
4×2	$N=3$	$J_\perp=1.0$	$Q_\perp=0.0$	$\beta_{\rm qmc}=32.0$	
$e_{\rm ex}$	-0.74157	$\rho^x_{\rm ex}$	0.043932	$\mathcal{O}^x_{\rm ex}$	0.030816
$e_{\rm qmc}$	$-0.74158(1)$	$\rho^x_{\rm qmc}$	0.043928(5)	$\mathcal{O}^x_{\rm qmc}$	0.030821(3)
4×2	$N=3$	$J_\perp=1.0$	$Q_\perp=1.0$	$\beta_{\rm qmc}=32.0$	
$e_{\rm ex}$	-1.25095	$\rho^x_{\rm ex}$	0.011196	$\mathcal{O}^x_{\rm ex}$	0.029878
$e_{\rm qmc}$	$-1.25095(2)$	$\rho^x_{\rm qmc}$	0.011199(2)	$\mathcal{O}^x_{\rm qmc}$	0.029878(2)

TABLE I: Test comparisons of measurements from exact diagonalization and finite-T QMC studies for the $N=2$ and $N=3$. The energies reported here are per site and the stiffness and VBS order parameters are defined in equations (9 , 10) and (12). For rectangular systems we have used the stiffness along the x-direction and VBS order parameter for x-oriented bonds. All systems have periodic boundary conditions.

For future reference, Table I contains test comparisons between measurements obtained from a SSE-QMC study and exact diagonalization (ED) on 4×4 and 4×2 systems with various $J_\perp$-$Q_\perp$ at $N=2$ and $N=3$. We list values for the ground state energy per site, spin stiffness as in Eqs. (9 , 10) as well as the VBS order parameter, defined in Eq. (12). For the rectangular systems we have indicated that we use the stiffness in the x-direction and VBS order parameter with x-oriented bonds.

Appendix B: $N=5$

Here we present a study of the SF-VBS phase transition at $N=5$, which also shows clear symptoms of first-order behavior. In Fig. 7 we show the SF-VBS crossings that allow us to determine the critical point. Unlike in the $N=2$ case, the position of the crossings drifts in the same direction from both the SF and VBS side. Taking finely binned data near the transition again shows us signs of first-order behavior.

In Fig. 8 we show history and histogram data for $N=5$. For our largest system size we are able to see significant evidence of a first order transition in both the history and histogram. We note here that unlike in the $N=2$ case, the location of the transition seems to drift

substantially with the system size. This results in only seeing clear signs of on-off switching (indicative of a first-order transition) for our largest system size, although it serves to illustrate the presence of a drift. It is arguably the case that the transition is weakening as a function of N given the less pronounced double peaks in the histograms.

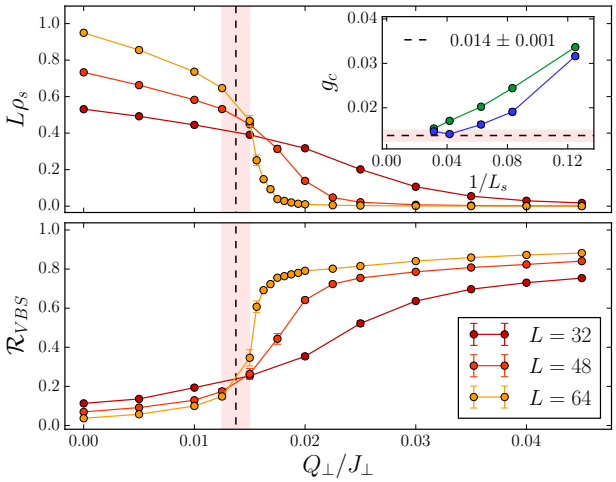

FIG. 7: Crossings at the SF-VBS quantum phase transition for $N = 5$ in $H^N_{J_\perp Q_\perp}$. The main panels shows the crossings for $L\rho_s$ and $\mathcal{R}_{VBS}$, which again show a direct transition between the superfluid and VBS states at $g_c = 0.014(1)$.

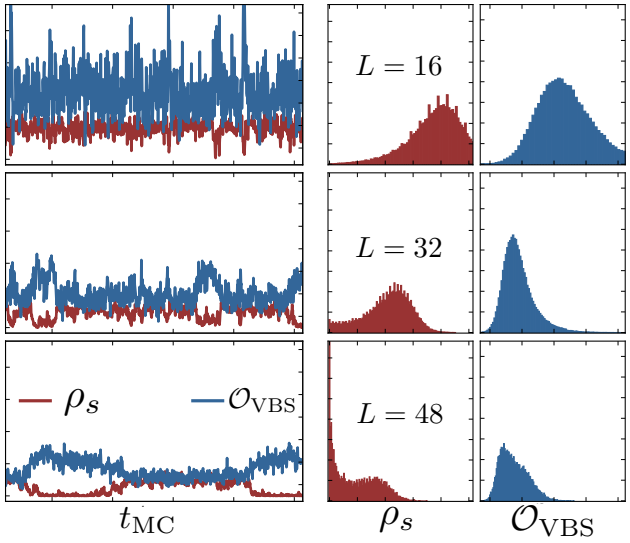

FIG. 8: Evidence for first order behavior at the SF-VBS quantum phase transition for $N = 5$. The data was collected at a coupling $g = 0.01875$. The left panel shows MC histories for both ρ_s and $\mathcal{O}_{VBS}$, with clear evidence for switching behavior characteristic of a first order transition at the largest system size $L = 48$. The right panel shows histograms of the same quantities with double peaked structure emerging at $L = 48$. Here we note that the location of the transition for each system size drifts more significantly than in the $N = 2$ case. Also it can be argued that the transition shows signs of weakening. Here we use a finer bin size for the histories (100 MC steps per point).